

Equilibrium planform of pocket beaches behind breakwater gaps: On the shape of the equilibrium shoreline

Ahmed I. Elshinnawy ^a, Raúl Medina ^b, Mauricio González ^b

^a Irrigation and Hydraulics Engineering Department, Faculty of Engineering, Tanta University, 31733, Tanta, Egypt

^b IHCantabria - Instituto de Hidráulica Ambiental de la Universidad de Cantabria, Avda. Isabel Torres, 15, 39011, Santander, Spain

Abstract

Bay beaches are common coastal landforms along the world's coastlines and have frequently been used as equilibrium coastal systems to mitigate erosion problems and stabilize coasts. Throughout the literature, several formulae can be found to obtain the static equilibrium planform (SEP) of such beaches on the leeward sides of single protruding headland structures. However, equations used to define SEP behind breakwater gaps are rare and based on a limited number of studies, especially when the obliquity angle (β) is large. This paper proposes a new formula for modelling the SEP of bay beaches that includes cases with planform shapes characterized by large obliquity angles ($\beta > 75^\circ$) for which the SEP is almost quasi-semicircular. The formula represents a general form of the parabolic bay shape equation (PBSE) with modified coefficients to alter the planform's curvature to be quasi-semicircular, mimicking the behavior of such bays in nature. The coefficients are expressed as functions of both the obliquity angle (β) and the curvature-adjustment angle (ϕ), which was determined based on field observations of the best-fitting SEP of 26 bay beaches with ($\beta > 75^\circ$) along the coasts of Spain, Portugal and Brazil. Additionally, 32 beach cases characterized by smaller obliquity angles ($\beta < 70^\circ$) were included in the derivation of the curvature adjustment angle, which was expressed as a function of (β). The model showed good results in modelling the SEP, with an RMSE of 0.90° obtained when estimating the planform's curvature-adjustment angle (ϕ) to obtain quasi-semicircular planform shapes for the prototype cases, confirming its utility as a valuable tool for engineering applications.

KEYWORDS:

Bay beaches; Static equilibrium shoreline; Breakwater gaps; Curvature adjustment angle; Large obliquity; Wave diffraction.

1. Introduction

Bay beaches represent coastal features that are common worldwide. Researchers have claimed that bay beaches occupy approximately 50% of the world's coastlines (Inman and Nordstrom, 1971). Extensive terminology has been used to describe such famous curved beaches, including pocket beaches (Yasso, 1965), spiral beaches (Krumbein, 1944; LeBlond, 1972), crenulate-shaped bays (Silvester and Ho, 1972; González and Medina, 2001; Weesakul et al., 2010), headland bay beaches (LeBlond, 1979; Short and Masselink, 1999; Klein and Menezes, 2001; Hsu et al., 2010) and embayed beaches (Elshinnawy et al., 2017; 2018a; Castelle et al., 2020). These curved bay beaches appear in various configurations and different sizes on both oceanic and coastal margins, on the leeward sides of natural rocky headlands and man-made breakwaters. Their stability has motivated coastal engineers to model their equilibrium planform shapes to mitigate shoreline erosion problems and to design new beaches for coastal stabilization purposes. The concept of an equilibrium planform is very useful for defining the final shape of a shoreline on a scale of multiple years (González et al., 2010; Elshinnawy et al., 2018b; 2018c).

According to Hsu et al. (2010), the planform shapes of bay beaches may be classified as being in states of static equilibrium, dynamic equilibrium and natural reshaping. A static-equilibrium bay beach is in a state in which the predominant waves break simultaneously around the whole bay periphery; hence, the net sediment transport rate produced by the littoral currents is almost negligible, and no littoral drift is required to maintain long-term stability (Hsu et al., 2010).

Throughout the literature, several empirical equations can be found to obtain the static equilibrium planform of pocket beaches on the leeward sides of protruding headlands or man-made breakwaters, e.g., the well-known parabolic bay shape equation (PBSE) proposed by Hsu and Evans (1989) and its modified versions (e.g., Tan and Chiew, 1994; Uda et al., 2010). Such formulations were originally derived to model the SEP of bay beaches behind single headland breakwaters. In other words, these previous models are valid for fully developed beaches with planforms characterized by shorelines containing a curved section as well as a straight segment. This means that the planform shape of each bay is dominated and controlled by a single breakwater. On the other hand, the formulae utilized to model and obtain the best-fitting SEP of bay beaches on the leeward sides of breakwater gaps are scarce in the literature and have been developed based on a limited number of case studies, see Dean (1979) and Silvester and Hsu (1997). A brief review of the existing models in the literature is described below.

Hsu and Evans (1989) derived the PBSE, a second-order polynomial equation derived by fitting the planforms of 27 mixed cases of prototype and model bays in static equilibrium, see Fig. 1, as follows:

$$\frac{R}{R_o} = C_0 + C_1 \left(\frac{\beta}{\theta}\right) + C_2 \left(\frac{\beta}{\theta}\right)^2 \quad (1)$$

where (R_o) is the length of the control line that joins the diffraction point to the down-coast control point (P_o); this line is inclined (β) to the tangent of the straight segment of the bay. The three C coefficients are functions of the obliquity angle (β), i.e., the angle between the control line and the incident wave front at the diffraction point. These C coefficients are mathematically expressed by fourth-order polynomials; see Raabe et al. (2010). The radius (R), measured from the tip of the headland breakwater, defines the location of the shoreline using the angle (θ) measured from the wave crest. The PBSE was originally derived for obliquity angles in the range of ($\beta = 22.5^\circ$ - 72°), see Hsu and Evans (1989) and the Coastal Engineering Manual (USACE, 2002).

Tan and Chiew (1994) stated that the original PBSE of Hsu and Evans (1989) did not take into consideration the tangential boundary condition at the down-coast control point (P_o) when ($R=R_o$) and ($\beta=\theta$). Consequently, they improved the accuracy of the PBSE by applying the following boundary conditions at (P_o):

$$C_0 + C_1 + C_2 = 1 \quad (2)$$

$$C_1 + 2C_2 = \beta \cot \beta \quad (3)$$

Accordingly, they proposed a new version of Eq. (1) by reducing the number of unknown coefficients from three to one (α), as follows:

$$\frac{R}{R_o} = (1 - \beta \cot \beta + \alpha) + (\beta \cot \beta - 2\alpha) \left(\frac{\beta}{\theta}\right) + \alpha \left(\frac{\beta}{\theta}\right)^2 \quad (4)$$

where (α) represents the C_2 coefficient in Eq. (4) and is a function of the obliquity angle (β). Tan and Chiew (1994) determined this parameter based on the measured shapes of the model beaches that were characterized by obliquity angles of ($\beta < 70^\circ$) for almost all the employed cases and proposed the following formula for the static-equilibrium condition:

$$\alpha = 0.277 - 0.0785 * 10^{\left(\frac{\beta\pi}{180}\right)} \quad (5)$$

Both Eqns. (1) and (4) were derived to model the SEP of a bay beach behind a single headland structure. In other words, these formulae are applicable only for the case of a wave

diffraction pattern generated by a single breakwater. When waves approach a gap, they diffract with another pattern, resulting in a different wave height gradient pattern on the leeward side of the gap that further results in a different equilibrium planform shape from the above-mentioned parabolic shape. For more details, see the Shore Protection Manual (SPM) (1984); Penny and Price (1952); Goda (1985) and Dean and Dalrymple (1991).

Silvester and Hsu (1997) stated that when waves traverse a breakwater gap, the planform differs from that represented by the parabolic shape obtained using Eqns. (1) and (4) and mainly characterizes arcs of circles. Therefore, they presented a set of curves for bays formed by breakwater gaps to obtain the maximum indentation ratio (Y/X_{total}), see Fig. 2. They also proposed the following expression for the case of waves approaching the gap at the normal angle:

$$X_{total} = 2r + B \quad (6)$$

where (B) is the gap width, (r) is the distance between the gap's center and the shoreline position at an angle (θ') and (X_{total}) is the total width of the bay beach, see Fig. 2. Eq. (6) is the same as the model proposed by Dean (1979), who stated that a full evaluation of this equation requires additional laboratory and field data. It should be noted that the maximum indentation ratio in the model of Silvester and Hsu (1997) cannot exceed the value of 0.5, i.e., (Y/X_{total}) ≤ 0.5 . In other words, this model cannot be applied for beach cases with (Y/X_{total}) > 0.5 .

The PBSE can be applied to properly obtain the best-fitting static equilibrium planform (SEP) of pocket beaches characterized by obliquity angles with values of ($\beta < 75^\circ$) behind gaps, as shown in Fig. 3a for two beaches at Llarga, Spain. However, when applying either Eqns. (1) or (4) to bay beaches with large obliquity angles ($\beta > 75^\circ$) to the leeward sides of breakwater gaps, all cases result in planform shapes that do not properly fit the actual SEP. This can be displayed in Fig. 3b for the beaches at Terramar and El Camison in Spain; both beaches are characterized by large obliquity angles ($\beta > 75^\circ$). As shown in Fig. 3b, the planform obtained by applying Eq. (4) is seaward of the actual shoreline position, i.e., it does not properly fit the SEP of the bay beaches. In other words, the best-fitting SEP is less curved than that obtained by applying Eq. (4). Moreover, the best-fitting SEP of both beaches result in maximum indentation ratios (Y/X_{total}) larger than 0.5, which differs from the results obtained when using the models of Dean (1979) and Silvester and Hsu (1997) with valid limits of (Y/X_{total}) ≤ 0.5 . Accordingly, the existing models found in the literature are applicable neither to check the stability of existing bays nor to design new beaches when ($\beta > 75^\circ$) and (Y/X_{total}) > 0.5 . Consequently, this inapplicability underscores the need for a new model to obtain the SEP of bay beaches on the leeward sides of breakwater gaps when ($\beta > 75^\circ$).

Accordingly, the main aim of this paper is to propose a new model that defines and best fits the equilibrium planform shapes of bay beaches behind breakwater gaps with large obliquity angles ($\beta > 75^\circ$) that corresponds to narrow gaps. The study hypothesizes that the SEP of such bays on the leeward sides of small gaps can be represented by employing a second-order polynomial form such as the PBSE with modified coefficients.

The paper is organized as follows: First, a general introduction to bay beaches and their stability, as well as a brief review of the existing models found in the literature, is presented. This is followed by a description of the methodology of the study and the employed tools, which are delineated in section (2); the study cases and the available data are given in section (3). The results obtained from field cases and a discussion of the results are given in section (4). Section (5) addresses the new proposed model. Finally, the main conclusions of the study are presented in section (6).

2. Methodology and tools

This study employs prototype cases of both natural and man-made bay beaches on the leeward sides of breakwater gaps with large obliquity angles to best fit the SEP of the field cases. For this purpose, long-time-series wave data in addition to some numerical tools were utilized. The work methodology can be summarized as follows:

- 1- Collection of field cases of bay beaches along the Iberian Peninsula and Brazilian coasts with specific conditions (static equilibrium behind breakwater gaps with planforms characterized by large obliquity angles ($\beta > 75^\circ$)).
- 2- Analyses of the directional wave climates at the breakwater gaps in addition to the bathymetric data and aerial vertical photos of the prototype cases.
- 3- Obtaining the best-fitting SEP of the selected bay beach cases.
- 4- Analysis of the results of the field cases.
- 5- Derivation of a new model that defines the SEP of pocket beach cases behind breakwater gaps with ($\beta > 75^\circ$).

Descriptions of the tools employed to apply the aforementioned methodology are given in the subsequent sections.

2.1 Coastal Modeling System (SMC)

The Coastal Modelling System (SMC) is a user-friendly software package developed by the University of Cantabria (UC) for the *Dirección General de Costas* (the State Coastal Office) of the Spanish Environmental Ministry, see González et al. (2007). It includes some numerical models that allow the formulations and methodologies proposed in different

manuals to be elaborated for application by the ministry to coastal projects. The latest version of the system (SMC 3.0) is structured in a manner that divides the numerical models and data into two main tools, namely, the SMC Model and SMC-Tools. The latter incorporates 3 modules, (a) IH-DATA, (b) IH-AMEVA and (c) IH-DYNAMICS, while the SMC Model includes both short-term and long-term modules for studies on timescales of hours to days and for studies on timescales of years, respectively, in addition to a terrain module (for further details, see González et al. (2007), Raabe et al. (2010), González et al. (2016) and Quetzalcóatl et al., 2019)).

The IH-DATA module (Gomes and Silva, 2014; González et al., 2016) has three databases. One is associated with time series of coastal waves called DOW (Downscaled Ocean Waves), (Camus et al., 2013). The other two databases are associated with sea-level time series: one is for astronomical tides, called GOT (Global Ocean Tides), see González et al. (2016), and the other is for storm surges or meteorological tides, called GOS (Global Ocean Surges), see Cid et al. (2014). The IH-AMEVA module is used to statistically analyze the IH-DATA module consisting of wave climates and sea level time series and, later, is used for the statistical characterization of the results. Finally, the IH-DYNAMICS module is used in the post processing stage to provide extensive data and results. It calculates the wave mean energy flux, littoral sediment transport, and run-up and flooding levels in addition to climate change impacts on the coast. More detailed information about the availability and access to the SMC, which is an open-source software, is provided on the following website: <http://smc.ihcantabria.es/SMC25/en/>.

The spectral wave model OLUCA-SP, encompassed in the short-term module of the SMC software, see González et al. (2007), and the DOW database of SMC-Tools were used in this study. The wave model was utilized to propagate the time series of the DOW data towards the breakwater gaps.

2.2 Wave propagation model

The spectral wave model OLUCA-SP is a combined refraction-diffraction model that was originally based on the REF/DIF 1 model (Kirby and Dalrymple, 1992) of the University of Delaware. It is based on a parabolic approximation of the mild slope equation that governs the refraction, diffraction and shoaling of water waves propagating over a gently sloping bathymetry. The model is suitable for determining wave fields in open coastal areas even in the presence of coastal structures. It is capable of modelling and reproducing most wave propagation processes, such as refraction, shoaling, and diffraction, as well as the forward scattering and dissipation of wave energy due to breaking and bed friction. The model can read both frequency and directional spectra directly from files or from a TMA frequency

spectrum (Bouws et al., 1985), together with the wrapped normal directional spreading function of Borgman (1984). Additional details are described in González et al. (2007).

3. Study cases and data

The selected bay beach cases as well as the available data sources used in the current study, including aerial vertical images of the selected beaches and bathymetric and wave data, are described in the subsequent sections.

3.1 Beach cases

This study employed and analyzed the planforms of 26 bay beaches at 14 locations along the coasts of Spain, Portugal and Brazil, as shown in Fig. 4. Beach selection was carefully conducted considering specific conditions; in particular, static-equilibrium bay beaches on the leeward sides of breakwater gaps that produce quasi-semicircular planform bay shapes characterized by large obliquity angles ($\beta > 75^\circ$) were selected. Moreover, an assessment of historical images of the planform shape of each bay beach was carried out to check that the planform was stable. At least five vertical aerial images of each selected beach case, obtained based on Google Earth imagery, were utilized for this assessment.

3.2 Bathymetric and wave data

Bathymetric data representing the coastal zones of Spain, Portugal and Brazil collected by the Environmental Hydraulics Institute (IHCantabria) were utilized in this study. These digitalized bathymetric data are incorporated in the IH-DATA module of the Coastal Modelling System (SMC) (González et al., 2007; González et al., 2016; Quetzalcóatl et al., 2019) for the littoral areas along the Iberian Peninsula as well as the Brazilian coastlines.

For wave data, the DOW (Downscaled Ocean Waves) database (Camus et al., 2013) was used in this study, representing a period of more than 70 years (from 1948 onwards). The DOW database is a historical reconstruction of coastal waves. In other words, it is a downscaled wave reanalysis product covering coastal zones from the Global Ocean Waves (GOW) database (Reguero et al., 2012). The GOW database was generated using the WAVEWATCH III model (Tolman, 2014) forced by (NCEP/NCAR) wind field reanalysis products (Kalnay et al., 1996) (for more details, see Reguero et al. (2012)). The GOW database was then directionally calibrated using satellite data to avoid biases and deviations in the results (for more details, see Minguez et al. (2011a)). This calibrated (GOW) dataset was used to select a representative subset of sea states in the deep-water region, guaranteeing that all possible conditions were represented, including extreme events, see Camus et al. (2011b). The selected sea states were propagated using the SWAN spectral wave model (Booij et al., 1999) with a

high spatial resolution over detailed bathymetries. Finally, time series of the propagated sea state parameters at each location were reconstructed, see Camus et al. (2011a). The DOW wave climate database contains available data covering the entire Spanish and Brazilian coasts with a spatial resolution of 0.01° (i.e., each 1 km) along the coastlines. It provides different wave parameters for each sea state (e.g., the significant wave height (H_s), spectral peak period (T_p), and mean wave direction (θ_m)) with a temporal resolution of one hour. More detailed information about the availability of and access to historical wind, wave and sea level data is provided on the following website: <http://www.ihdata.ihcantabria.com>.

3.3 Static equilibrium planform

For each bay beach among the cases selected for this study, data points close to the breakwater gap were obtained and selected from the DOW data time series. Furthermore, the wave climate was characterized by calculating the energy flux (EF) for each sea state as the product of the wave energy (E) and the group celerity (C_g) as follows:

$$EF = E * C_g = \frac{1}{16} * \rho * g * H_s^2 * C_g \quad (7)$$

where ρ is the water density, g is the gravitational acceleration, and H_s is the significant wave height for each sea state. Furthermore, the direction of the mean wave energy flux (θ_{EF}) was calculated for the whole wave climate as follows:

$$\theta_{EF} = \arctan \frac{EF_y}{EF_x} = \arctan \frac{\sum_{i=1}^n EF_i \sin \theta_i}{\sum_{i=1}^n EF_i \cos \theta_i} \quad (8)$$

where EF_i and θ_i are the value and the direction, respectively, of the wave energy flux for each sea state. This direction is recommended to represent the orientation of the wave front at the diffraction point for use in equilibrium planform studies of bay beaches, see González and Medina (2001), Hsu et al. (2010) and Elshinnawy et al. (2017; 2018a).

Moreover, following González et al. (2010) and Elshinnawy et al. (2018a), the spectral peak period (T_{p12}) associated with the significant wave height exceeding 12 hours each year (H_{s12}) was computed as a descriptor of the wave climate. This wave period was derived by plotting the probability density function (PDF) of the peak period associated with a range of values of the significant wave height within the domain of ($H_{s12} \pm 0.01$ m). Consequently, (T_{p12}) was obtained as the most probable peak period associated with the (H_{s12}) parameter. Additionally, the wavelength (L) was obtained as a function of the water depth at the breakwater gap (d) and of the wave period (T_{p12}). The characteristics of the selected beach cases as well as the calculated values of the above-mentioned parameters are listed in Table 1.

The best-fitting static equilibrium planform shapes of the selected bay beaches were plotted onto the corresponding aerial vertical images. The direction of the mean wave energy flux (θ_{EF}) at the breakwater gap was employed. Following Benedet et al. (2004) and Hsu et al. (2010), the best-fitting SEP of each bay beach was plotted starting from a down-coast control point close to the mid-width point of the gap. Consequently, the obliquity angle (β) was determined for each case. As listed in Table 1, the (β) values ranged from (75.8° – 86°) for the selected bay beaches with dimensionless gap widths in the domain of ($B/L = 0.4 - 2.63$). Fig. 5 shows plots of the best-fitting SEP of 3 bay beaches in Spain, Portugal and Brazil.

4. Results and discussion

The results obtained from the employed field cases as well as the discussion of the results are described in the subsequent sections.

4.1 Results

Based on the best-fitting SEP of the prototype bay beach cases employed in the current study, the radius (R_{180}) defining the location of the shoreline at an angle ($\theta = 180^\circ$) was determined for each case. The angle (θ) is measured from the wave crest corresponding to the direction of the mean wave energy flux (θ_{EF}) at the diffraction point, see Fig. 6. The results obtained from the field observations, as listed in Table 2, displayed a significant dependence of the radius (R_{180}) on the offshore distance (Y) between the diffraction point and the down-coast control point, and thus on the control length (R_o), see Fig. 6, leading to the following relationship:

$$\frac{R_{180}}{L} = 0.53 \left(\frac{Y}{L}\right)^{1.1} = 0.53 \left(\frac{R_o \sin \beta}{L}\right)^{1.1} \quad (9)$$

Fig. 7 shows the relationship between the dimensionless distances (R_{180}/L) and (Y/L), i.e., Eq. (9), which has an R^2 value of 0.97. The radius (R_{180}) was also computed by applying the model of Tan and Chiew (1994), i.e. Eq. (4), as listed in Table 2 (hereafter (R_{180})_{TS94}). When comparing the (R_{180}) values based on the best-fitting planform shapes and the (R_{180})_{TS94} values obtained using Eq. (4), it is clear that Eq. (4) underestimates the radius (R_{180}) of the actual shoreline position, whereas the ratio between these values [$R_{180}/(R_{180})_{TS94}$] is larger than 1.5 for all the beach cases. This means that the model of Tan and Chiew (1994) results in planform shapes located seaward of the actual equilibrium shorelines, i.e., this model is not valid for beach cases characterized by large obliquity angles ($\beta > 75^\circ$), as was previously shown in Fig. 3b.

Additionally, the maximum indentation ratio (Y/X_{total}) was determined based on the best-fitting SEP of the prototype cases. This ratio was also computed using the methodology of

Silvester and Hsu (1997), as listed in Table 2. When comparing the values of this indentation ratio based on the results of this study and the work of Silvester and Hsu (1997), it can be noticed that the maximum indentation ratio for the bay beaches with large obliquity angles ($\beta > 75^\circ$) is larger than 0.5 for all cases, which differs from the results of Dean (1979) and Silvester and Hsu (1997). Consequently, this confirms the need for a new model to obtain the SEP of semicircular bay beaches rather than using models found throughout the literature.

4.2 Discussion

The planform of a beach is mainly governed by the wave-induced currents that dictate the indentation of the embayed beach. Longshore currents may be generated due to wave height gradients as well as waves breaking obliquely with the equilibrium shoreline orientation (González and Medina, 2001; Elshinnawy et al., 2018b). Referring to Fig. 8 and according to González and Medina (2001), the SEP can be obtained as follows:

$$SEP = WFB - \int_{H_o}^{H_j} K_4 dH \quad (10)$$

where WFB is the wave front at breaking, dH represents the wave height gradients and K_4 is a coefficient that depends on the beach slope and the breaker index, see González and Medina (2001), who stated that K_4 could be assumed to be constant under static equilibrium conditions. This means that the SEP can be obtained from the position of the wave front at breaking minus a term that is proportional to the longitudinal wave height gradients. In other words, for static equilibrium conditions, the shoreline is solely controlled by the position of the WFB and the wave height gradients. Furthermore, the weaker the dH is, the more closely the SEP tends to follow the shape of the WFB.

Wave diffraction causes circular wave fronts and longitudinal wave height gradients due to the lateral spreading of energy from the illuminated (transition) zone to the shadow zone, see Fig. 8. In other words, zone (2) feeds zone (1) with dH , resulting in an SEP that is different from the position of the WFB, as illustrated by Eq. (10). This is the situation for wave diffraction at a single headland breakwater. However, in the case of a bay beach with a large obliquity angle ($\beta > 75^\circ$) behind a gap, the transition zone is quite narrow under most conditions, and thus, the wave height gradients are quite small, leading to a quasi-semicircular equilibrium planform following the WFB, i.e., following the diffracted circular wave front. In this context, the theory of wave diffraction through a gap, as introduced by Penny and Price (1952), is useful for understanding the wave height gradients applicable in such cases. These authors proposed the following formula to compute the diffraction coefficient (K_d) and thus the diffracted wave height behind breakwater gaps with dimensionless widths of ($B/L = 1-2$):

$$K_d = \frac{B}{\sqrt{LY}} \left[1 + \frac{\pi^2}{18L^2Y^2} \left(3x^2 + \frac{B^2}{4} \right) \right] \quad (11)$$

where (x) is the distance measured from the gap centerline towards the breakwaters of the gap, i.e., $(x=0)$, at the gap centerline). Referring to Eq. (11), Penny and Price (1952) stated that waves are nearly of uniform height $\left(\frac{B}{\sqrt{LY}}\right)$ along the whole gap width (B) , as the second term of the right-hand side of Eq. (11) is very small along the gap, see also Dean and Dalrymple (1991). This clarifies that the wave height gradients along the gap (dH) are very small within the narrow transition zone. As a result, the static equilibrium shoreline would follow the position of the circular WFB. This means that the SEP would be quasi-semicircular, i.e., different from the common parabolic planform shape located on the leeward side of a single breakwater. Accordingly, this explains the non-validity of both the PBSE of Hsu and Evans (1989) and the modified version of Tan and Chiew (1994) for bay beaches behind gaps with planforms characterized by large obliquity angles $(\beta > 75^\circ)$.

Fig. 9 reveals that, when utilizing Eq. (4), the larger the obliquity angle is, the larger the radius ratio (R_{180}/R_o) is up until a value of $(\beta = 75.8^\circ)$, at which point (R_{180}/R_o) reaches its maximum value of 0.3457. Then, this radius ratio decreases with the augmentation of the obliquity angle for the domain of $(\beta > 75.8^\circ)$, see Fig. 9. It is worth noting that this radius ratio slightly changes over the range of $(70^\circ < \beta < 85^\circ)$ with values of 0.343–0.3457. Physically, when applying Eq. (4) using large obliquity angles $(\beta > 75.8^\circ)$, the decrease in (R_{180}/R_o) for $(\beta > 75.8^\circ)$ would result in a planform shape that is located seaward of the actual shoreline's SEP, as previously shown in Fig. 3b. This agrees with the results of the current study and indicates that Eq. (4) cannot be used for modelling the SEP of bay beaches when $(\beta > 75^\circ)$, such as for beach cases located on the leeward sides of narrow breakwater gaps that produce large obliquity angles of the equilibrium planform. In other words, the presence of a gap modifies the diffraction pattern behind the gap, resulting in large obliquity angle values $(\beta > 75^\circ)$ of the equilibrium shoreline.

The coefficients of Eqns. (1) and (4) are implicitly dependent on the wave height gradients that are present when waves diffract at a single breakwater. However, when (dH) is too weak or negligible, new C coefficients that are independent of the wave height gradients are needed in the PBSE, leading to quasi-semicircular static equilibrium planforms. Accordingly, there is a need for a new model that satisfies this condition for bay beaches with planform shapes characterized by large obliquity angles.

5. Proposed model

Careful analysis of the geometry of the planform of a static equilibrium shoreline with ($\beta > 75^\circ$) behind a small gap shows that the planform obtained by applying Eq. (4) is more curved than the best-fitting SEP of the actual shoreline, see Fig. 6. In other words, the curvature of the planform produced by the original PBSE is larger than that of the best-fitting SEP. Mathematically, the second derivative, $f''(\beta/\theta)$, of the function $R/R_o = f(\beta/\theta)$, which is a function of the (C_2) coefficient of Eqns. (1) and (4), is expressed as follows, see Elshinnawy et al. (2018b):

$$f''\left(\frac{\beta}{\theta}\right) = 2C_2 = 2\alpha \quad (12)$$

This second derivative represents the curvature of the planform curved shape. Since the best-fitting SEP of the actual shoreline is less curved than that obtained with Eq. (4), the curvature of the best-fitting SEP must be smaller than that obtained with the original PBSE. In other words, the best-fitting SEP must have a larger (α) parameter value, i.e. with fewer negative values, than that computed using Eq. (5). This could be achieved by reducing the power of the second term on the right-hand side of Eq. (5) to decrease the curvature of the planform. As a result, a new coefficient (α_{gap}) can be expressed as follows:

$$\alpha_{gap} = 0.277 - 0.0785 * 10^{\left(\frac{(\beta-\phi)\pi}{180}\right)} \quad (13)$$

where (ϕ) is the *curvature-adjustment angle* that alters the planform's curvature to obtain the best-fitting SEP. It is worth clarifying that the (α) parameter calculated using Eq. (5) has values between -1 and -2 for obliquity angles between ($\beta = 70^\circ$) and ($\beta = 85^\circ$), respectively. Moreover, the beach cases employed by Tan and Chiew (1994) to derive Eq. (5) had only one beach case with ($\beta > 70^\circ$), which increased the uncertainty in applying Eq. (5) for bay beaches characterized by ($\beta > 70^\circ$). Accordingly, Eq. (13) is proposed to reduce the negative values of the (α) parameter, i.e. by decreasing the curvature of the planforms of pocket beaches with ($\beta > 70^\circ$) to obtain the actual best-fitting SEP shapes existing in nature.

To mathematically express the (ϕ) angle for a larger domain of the obliquity angle (β), 32 static equilibrium bay beaches characterized by ($\beta < 70^\circ$) on the leeward sides of breakwater gaps were also included in the derivation of the curvature adjustment angle (ϕ). These 32 beach cases are located along the Spanish coast, and their SEP shapes were best fitted using Eq. (4), see Fig. 3a. In other words, they all have ($\phi = 0$). The obliquity angle values of these beach cases are listed in Table 3. Based on the results obtained for the 26 prototype pocket beaches and their best-fitting SEP and by adding the data of 32 cases with ($\phi = 0$), the (ϕ)

angle was determined to be a function of the obliquity angle. Fig. 10 shows the relationship between the curvature-adjustment angle (ϕ) and the obliquity angle (β), where the best-fit line has the following mathematical expression:

$$\phi = \left(\frac{19}{(1+e^{-0.3(\beta-45)})^{8270}} \right) \quad (14)$$

Fig. 10 displays a trend in which the larger the obliquity angle (β) is, the larger the curvature adjustment angle (ϕ) is. Eq. (14) was derived based on a regression analysis of the results obtained from field observations of the best-fitting SEP of 26 bay beaches with large obliquity angles ($\beta > 75^\circ$) behind breakwater gaps and by employing the 32 beach cases with ($\phi=0$) for ($\beta < 70^\circ$). This formula has a root mean square error (RMSE) of 0.90° in the estimation of the (ϕ) angle when ($\beta > 75^\circ$). Eq. (14) exemplifies the beach-curvature adjustment for cases with large obliquity angles ($\beta > 70^\circ$), where ($\phi > 0$). Moreover, this equation results in ($\phi=0$) for bay beaches characterized by ($\beta < 70^\circ$). Accordingly, the (α_{gap}) parameter, given by Eq. (13), could be computed. The values of the abovementioned parameters obtained based on the best-fitting SEP shapes of the 26 cases with ($\beta > 75^\circ$) are listed in Table 4.

The two curves shown in Fig. 6 start at the same down-coast control point (P_o) and have the same obliquity angle (β), fulfilling the tangential boundary condition at that point. Therefore, the gradient or the rate of change given as the first derivative of Eq. (4) would be identical for both curves, with a value of ($\beta \cot \beta$) for bay beaches under static equilibrium conditions, see Tan and Chiew (1994) and Elshinnawy et al. (2018b). Accordingly, the three C coefficients of the proposed PBSE version are expressed as follows:

$$C_{on} = 1 - \beta \cot \beta + \alpha_{gap} \quad (15)$$

$$C_{1n} = \beta \cot \beta - 2\alpha_{gap} \quad (16)$$

$$C_{2n} = \alpha_{gap} \quad (17)$$

Hence, the new proposed model can be rewritten as follows:

$$\frac{R}{R_o} = (1 - \beta \cot \beta + \alpha_{gap}) + (\beta \cot \beta - 2\alpha_{gap}) \left(\frac{\beta}{\theta} \right) + \alpha_{gap} \left(\frac{\beta}{\theta} \right)^2 \quad (18)$$

It is worth noting that when ($\phi = 0$) for the domain of ($\beta < 70^\circ$) and is substituted into Eq. (13), Eq. (18) gives the same results as the model of Tan and Chiew (1994) for bay beaches in static equilibrium, i.e. Eq. (4). Accordingly, the new proposed model, i.e. Eq. (18), can be

considered a general version of the PBSE that is valid and applicable for modelling the static equilibrium planform of bay beaches, including those characterized by ($\beta > 75^\circ$) on the leeward sides of breakwater gaps.

Fig. 11 displays the values of the (α_{gap}) parameter as a function of the obliquity angle (β) for the 26 beach cases with ($\beta > 75^\circ$). The points represent the results of the best-fitting SEP obtained from the field observations, whereas the line represents the proposed formula defined by Eq. (13). Referring to Fig. 9 and Eq. (9), the results of the best-fitting SEP shapes of the beach cases displayed the dependence of the radius ratio (R_{180}/R_o) on the obliquity angle (β). Fig. 11 shows that the behavior of the (α_{gap}) parameter shares the same pattern of the behavior of (R_{180}/R_o); these parameters change slightly with (β) for the domain of ($\beta > 70^\circ$), see Fig. 9. The value of the (α_{gap}) parameter changes between -0.79 and -1 for ($\beta > 75^\circ$), in contrast to the findings of Tan and Chiew (1994) regarding a significant change in (α) for ($\beta > 70^\circ$). This is in accordance with the results of Hsu and Evans (1989), who showed that the C_2 coefficient of Eq. (1) undergoes a slight, smooth change with the obliquity angle when ($\beta > 70^\circ$). Accordingly, the new proposed model, Eq. (13) and thus Eq. (18), has the merits of fulfilling both the tangential boundary condition at the down-coast control point (Tan and Chiew, 1994) and the behavior of the (C_2) coefficient of the original PBSE of Hsu and Evans (1989) for large obliquity angles ($\beta > 70^\circ$).

Fig. 12 shows two examples of the best-fitting SEP shapes as well as the shapes of the static-equilibrium shorelines when applying Eq. (18) for the beaches at Mogan and La Pinta, Spain; these beaches are characterized by large obliquity angles ($\beta > 75^\circ$). The plots reveal that the new model, Eq. (18), properly fits the quasi-semicircular SEP for these pocket beaches behind breakwater gaps when the obliquity angles are large ($\beta > 75^\circ$).

In summation, Eq. (18) can be used as a solution that satisfies Eq. (10) when the SEP tends to follow the WFB. The formula plots the position of the shoreline, modifying its curvature, by introducing the (α_{gap}) parameter to reduce the curvature of the quasi-semicircular planform. The new model adjusted the planform's curvature through the adjustment angle (ϕ), which, in turn, altered the C coefficients of the PBSE. Eq. (18) is applicable for modelling the SEP of pocket beaches, including cases characterized by large obliquity angles for the domain ($\beta > 75^\circ$), by employing the direction of the mean wave energy flux (θ_{EF}) at the diffraction point to obtain a quasi-semicircular SEP. Moreover, the new proposed model could be used to design new beaches for shore protection with the presence of enough sediment available for the formation of the coastline.

6. Conclusion

Equilibrium bay beaches have been widely used to mitigate shoreline erosion problems and stabilize coasts. These beaches may exist under static or dynamic equilibrium conditions. Throughout the literature, although several empirical formulae have been derived to model the best-fitting static equilibrium planform (SEP) of bay beaches on the leeward sides of single headland breakwaters, equations used to define SEP behind breakwater gaps are rare, especially for bays in which the obliquity angle is large ($\beta > 75^\circ$). This condition corresponds to narrow breakwater gaps in most conditions. A new formula, Eq. (18), was derived to plot and best-fit the SEP of bay beaches characterized by large obliquity angles ($\beta > 75^\circ$). The formula has the same form as the parabolic bay shape equation (PBSE); the C coefficients of the PBSE were modified through the introduction of the curvature-adjustment angle (ϕ) in the C_2 coefficient, i.e. the (α_{gap}) parameter of Eq. (18), to decrease the curvature of the planform. This reduction in the curvature of the SEP resulted in the best-fit equilibrium planform shape for quasi-semicircular bays in nature, for which the wave height gradients are so small that the SEP tends to follow the diffracted circular wave front at breaking (WFB). The derivations of Eqns. (13) and (14) to obtain the (ϕ) angle and thus the (α_{gap}) parameter of the proposed model, i.e. Eq. (18), were carried out based on field observations of the best-fitting SEP of 26 prototype bay beaches characterized by ($\beta > 75^\circ$) along the Iberian Peninsula and the Brazilian coasts and including 32 cases with smaller obliquity angles ($\beta < 70^\circ$). Eq. (14) computes the (ϕ) angle for bay beaches characterized by ($\beta > 75^\circ$), resulting in ($\phi = 0$) for the domain of ($\beta < 70^\circ$). The new formula showed good results in defining the SEP of small gap bay beaches, with an RMSE = 0.90° in the estimation of the (ϕ) angle when ($\beta > 75^\circ$). The results reveal an altered curvature of the SEP of both natural and man-made bay beaches. The model could be used as a general formula to design new bay beaches in static equilibrium conditions, including bays on the leeward sides of breakwater gaps when ($\beta > 75^\circ$) with the presence of enough sediment available for the formation of the coastline. Moreover, the model could be utilized for stability studies of pocket beaches in static equilibrium conditions.

Acknowledgements

The authors would like to acknowledge the support of the Spanish Ministry of Economy, Industry, and Competitiveness under Grant BIA2017–89491-R (Beach-Art Project). The authors would also like to thank the reviewers for their valuable suggestions and comments.

References

- Benedet, L., Klein, A.H.F., Hsu, J.R.C., 2004. Practical insights and applicability of empirical bay shape equations. Proc. 29th Inter. Conf. Coastal Eng., vol. 2. ASCE, pp. 2181–2193.
- Booij, N., Ris, R.C., Holthuijsen, L.H., 1999. A third-generation wave model for coastal regions. I- Model description and validation. J. Geophys. Res. 104, 7649–7666. <https://doi.org/10.1029/98jc02622>
- Borgman, L.E., 1984. Directional Spectrum Estimation for the S_{xy} Gauges. Technical Report CERC, Waterways Experiment Station, Vicksburg, Miss, pp. 1–104.
- Bouws, E., Günther, H., Rosenthal, W., Vincent, C.L., 1985. Similarity of the wind wave spectrum in finite depth water: 1. Spectral form. J. Geophys. Res. Ocean. 90, 975–986. <https://doi.org/10.1029/JC090iC01p00975>
- Camus, P., Mendez, F.J., Medina, R., 2011a. A hybrid efficient method to downscale wave climate to coastal areas. Coast. Eng. 58, 851–862. <https://doi.org/10.1016/j.coastaleng.2011.05.007>
- Camus, P., Mendez, F.J., Medina, R., Cofiño, A.S., 2011b. Analysis of clustering and selection algorithms for the study of multivariate wave climate. Coast. Eng. 58, 453–462. <https://doi.org/10.1016/j.coastaleng.2011.02.003>
- Camus, P., Mendez, F.J., Medina, R., Tomas, A., Izaguirre, C., 2013. High resolution downscaled ocean waves (DOW) reanalysis in coastal areas. Coast. Eng. 72, 56–68. <https://doi.org/10.1016/j.coastaleng.2012.09.002>
- Castelle, B., Robinet, A., Idier, D., D’Anna, M., 2020. Modelling of embayed beach equilibrium planform and rotation signal. Geomorphology 369, 107367. <https://doi.org/10.1016/j.geomorph.2020.107367>
- Cid, A., Castanedo, S., Abascal, A.J., Menéndez, M., Medina, R., 2014. A high resolution hindcast of the meteorological sea level component for Southern Europe: the GOS dataset. Clim. Dyn. 1–18. <https://doi.org/10.1007/s00382-013-2041-0>
- Dean, R.G., 1979. Diffraction Calculation of Shoreline Planforms. Proc. Coast. Eng. Conf. 2, 1903–1917. <https://doi.org/10.9753/icce.v16.115>
- Dean, R.G., Dalrymple, R.A., 1991. Water Wave Mechanics for Engineers and Scientists. Advanced Series on Ocean Engineering, vol.2. World Scientific, Singapore (371 pp).

- Elshinnawy, A.I., Medina, R., González, M., 2017. On the relation between the direction of the wave energy flux and the orientation of equilibrium beaches. *Coast. Eng.* 127, 20–36. <https://doi.org/10.1016/j.coastaleng.2017.06.009>
- Elshinnawy, A.I., Medina, R., González, M., 2018a. On the influence of wave directional spreading on the equilibrium planform of embayed beaches 133, 59–75. <https://doi.org/10.1016/j.coastaleng.2017.12.009>
- Elshinnawy, A.I., Medina, R., González, M., 2018b. Dynamic equilibrium planform of embayed beaches: Part 1. A new model and its verification. *Coast. Eng.* 135, 112–122. <https://doi.org/10.1016/j.coastaleng.2018.01.010>
- Elshinnawy, A.I., Medina, R., González, M., 2018c. Dynamic equilibrium planform of embayed beaches: Part 2. Design procedure and engineering applications. *Coast. Eng.* 135, 123–137. <https://doi.org/10.1016/j.coastaleng.2018.01.001>
- Goda, Y., 1985. *Random Seas and Design of Maritime Structures*. University of Tokyo Press, Tokyo, Japan, 462 pp.
- Gomes, G.Da., da Silva, A.C., 2014. Coastal Erosion Case at Candeias Beach (NE-Brazil). *J. Coast. Res.* 71, 30–40. <https://doi.org/10.2112/SI71-004.1>
- González, M., Medina, R., 2001. On the application of static equilibrium bay formulations to natural and man-made beaches. *Coast. Eng.* 43, 209–225. [https://doi.org/10.1016/S0378-3839\(01\)00014-X](https://doi.org/10.1016/S0378-3839(01)00014-X)
- González, M., Medina, R., Gonzalez-Ondina, J., Osorio, A., Méndez, F.J., García, E., 2007. An integrated coastal modeling system for analyzing beach processes and beach restoration projects, *SMC. Comput. Geosci.* 33, 916–931. <https://doi.org/10.1016/j.cageo.2006.12.005>
- González, M., Medina, R., Losada, M., 2010. On the design of beach nourishment projects using static equilibrium concepts: Application to the Spanish coast. *Coast. Eng.* 57, 227–240. <https://doi.org/10.1016/j.coastaleng.2009.10.009>
- González, M., Nicolodi, J.L., Quetzalcóatl, O., Cánovas, V., Hermosa, A.E., 2016. Brazilian coastal processes: wind, wave climate and sea level, 2016. In: Short, A.D., Klein, A.H. da F. (Eds.), *Brazilian Beach Systems*, Coastal Research Library 17. Springer, pp. 37–66. https://doi.org/10.1007/978-3-319-30394-9_2. ISBN 978-3-319-30392-5.

- HSU, J.R.C., EVANS, C., 1989. Parabolic Bay Shapes and Applications. *Proc. Inst. Civ. Eng.* 87, 557–570. <https://doi.org/10.1680/iicep.1989.3778>
- Hsu, J.R.C., Yu, M.J., Lee, F.C., Benedet, L., 2010. Static bay beach concept for scientists and engineers: A review. *Coast. Eng.* 57, 76–91. <https://doi.org/10.1016/j.coastaleng.2009.09.004>
- Inman, D.L., Nordstrom, C.F., 1971. On the tectonic and morphologic classification of coasts. *J. Geol.* 79, 1–21.
- Kalnay, E., Kanamitsu, M., Kistler, R., Collins, W., Deaven, D., Gandin, L., Iredell, M., Saha, S., White, G., Woollen, J., Zhu, Y., Chelliah, M., Ebisuzaki, W., Higgins, W., Janowiak, J., Mo, K.C., Ropelewski, C., Wang, J., Leetmaa, A., Reynolds, R., Jenne, R., Joseph, D., 1996. The NCEP/NCAR 40-year reanalysis project. *Bull. Am. Meteorol. Soc.* [https://doi.org/10.1175/1520-0477\(1996\)077<0437:TNYRP>2.0.CO;2](https://doi.org/10.1175/1520-0477(1996)077<0437:TNYRP>2.0.CO;2)
- Kirby, J.T., Dalrymple, R.A., 1992. Combined Refraction/diffraction Model REF/DIF 1, Version 2.4. Documentation and User's Manual. Research Report CACR-92-04. Center for Applied Coastal Research, University of Delaware.
- Klein, A.H.F., Menezes, J.T., 2001. Beach morphodynamics and profile sequence for a headland bay coast. *J. Coast Res.* 17 (4), 812–835.
- Krumbein, W.C., 1944. Shore Processes and Beach Characteristics. Technical Memorandum, vol.3. Beach Erosion Board, U.S. Army Corps of Engineers, p. 47.
- LeBlond, P.H., 1972. On the formation of spiral beaches. In: *Proc. 13th Inter. Conf. Coastal Eng.*, vol. 2. ASCE, pp. 1331–1345.
- LeBlond, P.H., 1979. An explanation of the logarithmic spiral plan of headland bay beaches. *J. Sediment. Petrol.* 49, 1093–1100.
- Mínguez, R., Espejo, A., Tomás, A., Méndez, F.J., Losada, I.J., 2011. Directional calibration of wave reanalysis databases using instrumental data. *J. Atmos. Ocean. Technol.* 28, 1466–1485. <https://doi.org/10.1175/JTECH-D-11-00008.1>
- Penny, W.G., Price, A.T., 1952. The diffraction theory of sea waves and the shelter afforded by breakwaters. *Philos. Trans. Roy. SOCA.* 244 (882), 236–253. <https://doi.org/10.1098/rsta.1952.0003>.

- Quetzalcóatl, O., González, M., Cánovas, V., Medina, R., Espejo, A., Klein, A., Tessler, M.G., Almeida, L.R., Jaramillo, C., Garnier, R., Kakeh, N., González-Ondina, J., 2019. SMCε, a coastal modeling system for assessing beach processes and coastal interventions: Application to the Brazilian coast. *Environ. Model. Softw.* 116, 131–152. <https://doi.org/10.1016/j.envsoft.2019.03.001>
- Raabe, A.L.A., Klein, A.H. da F., González, M., Medina, R., 2010. MEPBAY and SMC: Software tools to support different operational levels of headland-bay beach in coastal engineering projects. *Coast. Eng.* 57, 213–226. <https://doi.org/10.1016/j.coastaleng.2009.10.008>
- Reguero, B.G., Menéndez, M., Méndez, F.J., Mínguez, R., Losada, I.J., 2012. A Global Ocean Wave (GOW) calibrated reanalysis from 1948 onwards. *Coast. Eng.* 65, 38–55. <https://doi.org/10.1016/j.coastaleng.2012.03.003>
- Short, A.D., Masselink, G., 1999. Embayed and structurally controlled beaches. In: Short, A.D. (Ed.), *Handbook of Beach and Shore Face Morphodynamics*. John Willey & Sons, New York, pp. 230–249.
- Silvester, R., Ho, S.K., 1972. Use of crenulate shaped bays to stabilize coasts. In: *Proc. 13th Inter. Conf. Coastal Eng.*, vol. 2, pp. 1347–1365. ASCE. <https://doi.org/10.9753/icce.v13.%25p>.
- Silvester, R., Hsu, J.R.C., 1997. *Coastal stabilization*. Advanced Series on Ocean Engineering 14. World Scientific.
- Tan, S.K., Chiew, Y.M., 1994. Analysis of bayed beaches in static equilibrium. *J. Waterw. Port, Coast. Ocean Eng.* - ASCE 120, 145–153. [https://doi.org/10.1061/\(ASCE\)0733-950X\(1994\)120:2\(145\)](https://doi.org/10.1061/(ASCE)0733-950X(1994)120:2(145))
- Tolman, H., 2014. *User Manual and System Documentation of WAVEWATCH III Version 4.18 NOAA/NWS/NCEP/MMAB Technical Note 316*.
- Uda, T., Serizawa, M., Kumada, T., Sakai, K., 2010. A new model for predicting three dimensional beach changes by expanding Hsu and Evans' equation. *Coast Eng.* 57, 194–202. <https://doi.org/10.1016/j.coastaleng.2009.10.006>.
- USACE, 1984. *Shore Protection Manual*, 4ed, vol. 1. Waterways Experiment Station, Corps of Engineers, Washington DC, USA, p. 608.

- USACE (U.S. Army Corps of Engineers), 2002. Coastal Engineering Manual (Online).
USACE, Coastal Engineering Research Center, Washington, DC.
- Weesakul, S., Rasmeemasuang, T., Tasaduak, S., Thaicharoen, C., 2010. Numerical modeling of crenulate bay shape. *Coast Eng.* 57, 184–193. <https://doi.org/10.1016/j.coastaleng.2009.10.005>.
- Yasso, W.E., 1965. Plan geometry of headland bay beaches. *J. Geol.* 73, 702–714.
<http://www.journals.uchicago.edu/doi/10.1086/627111>.

TABLES

Table 1. Summary of static-equilibrium bay beaches and wave climate parameters.

No.	Beach	Location	d (m)	T_{p12} (sec)	θ_{EF} (°)	Y	Y/L	B	B/L	β (°)
1	Terramar 1	Spain	2.5	11	155	102	1.92	21	0.4	86
2	Terramar 2	Spain	2.5	11	155	84	1.57	21	0.4	81
3	La Concha 1	Spain	10	15.2	330	1029	7.04	384	2.63	78
4	La Concha 2	Spain	10	15.2	330	1009	6.90	384	2.63	81
5	Arenal den Castell 1	Spain	3	9.22	358	393	8.1	113	2.32	82.5
6	Arenal den Castell 2	Spain	3	9.22	358	251	5.14	113	2.32	75.8
7	Anfora 1	Spain	3	7	206	115	3.17	42	1.18	77
8	Anfora 2	Spain	3	7	206	167	4.58	42	1.18	85
9	Blanca	Spain	9.4	12.2	220	125	1.11	48.5	0.44	78.5
10	Amadores 1	Spain	10.57	8.08	238	216	2.95	93.5	1.27	77.6
11	Amadores 2	Spain	10.57	8.08	238	206	2.81	93.5	1.27	77.6
12	El Camison 1	Spain	3	7.46	193	214	5.44	100	2.54	76.2
13	El Camison 2	Spain	3	7.46	193	214	5.44	100	2.54	77
14	La Pinta 1	Spain	2.5	8.85	278	118	2.76	53	1.24	78.8
15	La Pinta 2	Spain	2.5	8.85	278	114	2.66	53	1.24	79.7
16	Las Americas-El Bobo	Spain	3	8.75	276	143	3.13	58	1.27	79.7
17	Mogan 1	Spain	3.4	8.34	188	116	2.49	48.5	1.04	78.6
18	Mogan 2	Spain	3.4	8.34	188	130	2.79	48.5	1.04	79
19	Sao Martinho do Porto 1	Portugal	8.5	14.9	320	830	6.33	214	1.61	83
20	Sao Martinho do Porto 2	Portugal	8.5	14.9	320	812	6.13	214	1.61	83
21	Janga 1	Brazil	2	7.91	109	146	4.26	54	1.57	80
22	Janga 2	Brazil	2	7.91	109	148	4.31	54	1.57	79.6
23	Janga 3	Brazil	2	8.1	119	161	4.6	50	1.42	81.2
24	Janga 4	Brazil	2	8.1	119	156	4.44	50	1.42	81.5
25	Janga 5	Brazil	2	8.04	95	204	5.85	53.5	1.54	83
26	Janga 6	Brazil	2	8.04	95	202	5.8	53.5	1.54	83

Table 2. Results of the radius (R_{180}) and the maximum indentation ratio based on the best-fitting SEP of prototype bay beach cases and the models of Tan and Chiew (1994) and Silvester and Hsu (1997).

No.	Beach	β (°)	R_{180}	* (R_{180}) _{TS94}	$R_{180}/$ (R_{180}) _{TS94}	X_{total}	Y	Y/X_{total}	** (Y/X_{total}) _{SH97}
1	Terramar 1	86	66.5	35.15	1.89	136	102	0.75	0.48
2	Terramar 2	81	48.5	29.4	1.74	136	84	0.62	0.475
3	La Concha 1	78	575.6	363	1.64	1614	1029	0.64	0.42
4	La Concha 2	81	663.4	352	1.88	1614	1009	0.62	0.42
5	Arenal den Castell 1	82.5	253.2	136.5	1.85	489	393	0.80	0.48
6	Arenal den Castell 2	75.8	123.8	89.5	1.51	489	251	0.51	0.475
7	Anfora 1	77	60	41	1.69	215	115	0.536	0.48
8	Anfora 2	85	111.8	57.6	1.94	215	167	0.77	0.485
9	Blanca	78.5	82	44.1	1.86	228	125	0.55	0.43
10	Amadores 1	77.6	133	76.6	1.74	351	216	0.62	0.41
11	Amadores 2	77.6	126	73	1.73	351	206	0.59	0.41
12	El Camison 1	76.2	118	76.2	1.64	337	214	0.63	0.40
13	El Camison 2	77	119	76	1.66	337	214	0.63	0.40
14	La Pinta 1	78.8	75	41.7	1.80	204	118	0.58	0.415
15	La Pinta 2	79.7	77	40.1	1.91	204	114	0.56	0.415
16	Las Americas-El Bobo	79.7	87	50.1	1.73	184	143	0.776	0.445
17	Mogan 1	78.6	72	41	1.76	203	116	0.57	0.435
18	Mogan 2	79	83	45.8	1.82	203	130	0.64	0.44
19	Sao Martinho do Porto 1	83	593	291.2	2.03	1320	830	0.63	0.445
20	Sao Martinho do Porto 2	83	516	281.7	1.83	1320	812	0.62	0.445
21	Janga 1	80	81	51.3	1.65	216	146	0.68	0.425
22	Janga 2	79.6	81	52	1.61	216	148	0.69	0.425
23	Janga 3	81.2	98.2	56.3	1.74	244	161	0.66	0.435
24	Janga 4	81.5	96	54.4	1.76	244	156	0.64	0.435
25	Janga 5	83	135.6	70.8	1.92	324	204	0.63	0.44
26	Janga 6	83	135	70.2	1.92	324	202	0.62	0.44

* The radius (R_{180}) based on the model of Tan and Chiew (1994)

**Maximum indentation ratio based on the model of Silvester and Hsu (1997)

Table 3. Additional beach cases characterized by ($\beta < 70^\circ$) and included in the regression analysis for the derivation of Eq. (14).

No.	Beach	β ($^\circ$)	ϕ ($^\circ$)
1	Palamos 1	68.4	Zero for all cases
2	Palamos 2	69	
3	Llarga 1	66	
4	Llarga 2	70	
5	Llarga 3	65	
6	Llarga 4	68	
7	Llarga 5	59	
8	Llarga 6	57	
9	Cubelles	57.2	
10	Cunit 1	69.8	
11	Cunit 2	67.7	
12	Cunit 3	64.7	
13	Mar de Cunit	65.4	
14	Cambrils	62	
15	Far del Forat 1	63.4	
16	Far del Forat 2	66	
17	Las Fuentes	66.5	
18	Benicassim 1	66.7	
19	Benicassim 2	61.6	
20	El Palo 1	59	
21	El Palo 2	51.3	
22	El Palo 3	56.6	
23	El Palo 4	58.2	
24	Bonita 1	66.6	
25	Bonita 2	56.5	
26	Nueva Andalucia 1	69.3	
27	Nueva Andalucia 2	68.5	
28	Nueva Andalucia 3	62.7	
29	Fuengirola	67.1	
30	Capobino	58.9	
31	Las Americas 1	68	
32	Las Americas 2	67.2	

Table 4. Results of the best-fitting SEP of field cases characterized by ($\beta > 75^\circ$).

No.	Beach	β ($^\circ$)	ϕ ($^\circ$)	α_{gap}
1	Terramar 1	86	18	-0.924
2	Terramar 2	81	16	-0.791
3	La Concha 1	78	13	-0.813
4	La Concha 2	81	16.5	-0.771
5	Arenal den Castell 1	82.5	16.5	-0.837
6	Arenal den Castell 2	75.8	8.5	-0.894
7	Anfora 1	77	10.5	-0.86
8	Anfora 2	85	17.5	-0.89
9	Blanca	78.5	14	-0.772
10	Amadores 1	77.6	13	-0.783
11	Amadores 2	77.6	12.6	-0.792
12	El Camison 1	76.2	10.2	-0.837
13	El Camison 2	77	10.6	-0.852
14	La Pinta 1	78.8	14.2	-0.776
15	La Pinta 2	79.7	15	-0.778
16	Las Americas-El Bobo	79.7	14	-0.821
17	Mogan 1	78.6	14.6	-0.75
18	Mogan 2	79	15	-0.75
19	Sao Martinho do Porto 1	83	18.5	-0.772
20	Sao Martinho do Porto 2	83	17	-0.837
21	Janga 1	80	13	-0.879
22	Janga 2	79.6	13	-0.863
23	Janga 3	81.2	14.5	-0.867
24	Janga 4	81.5	15	-0.86
25	Janga 5	83	16.9	-0.837
26	Janga 6	83	16.9	-0.837

FIGURES

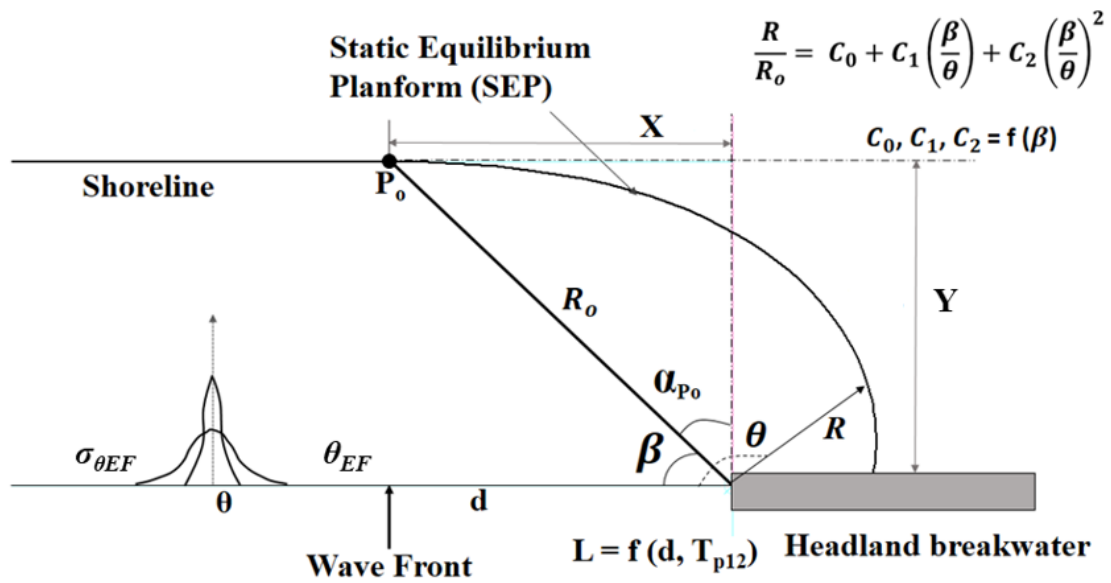


Fig. 1 Definition sketch of the parabolic bay shape equation (PBSE) for a bay beach in static equilibrium on the leeward side of a single headland breakwater proposed by Hsu and Evans (1989), modified from Elshinnawy et al. (2018a).

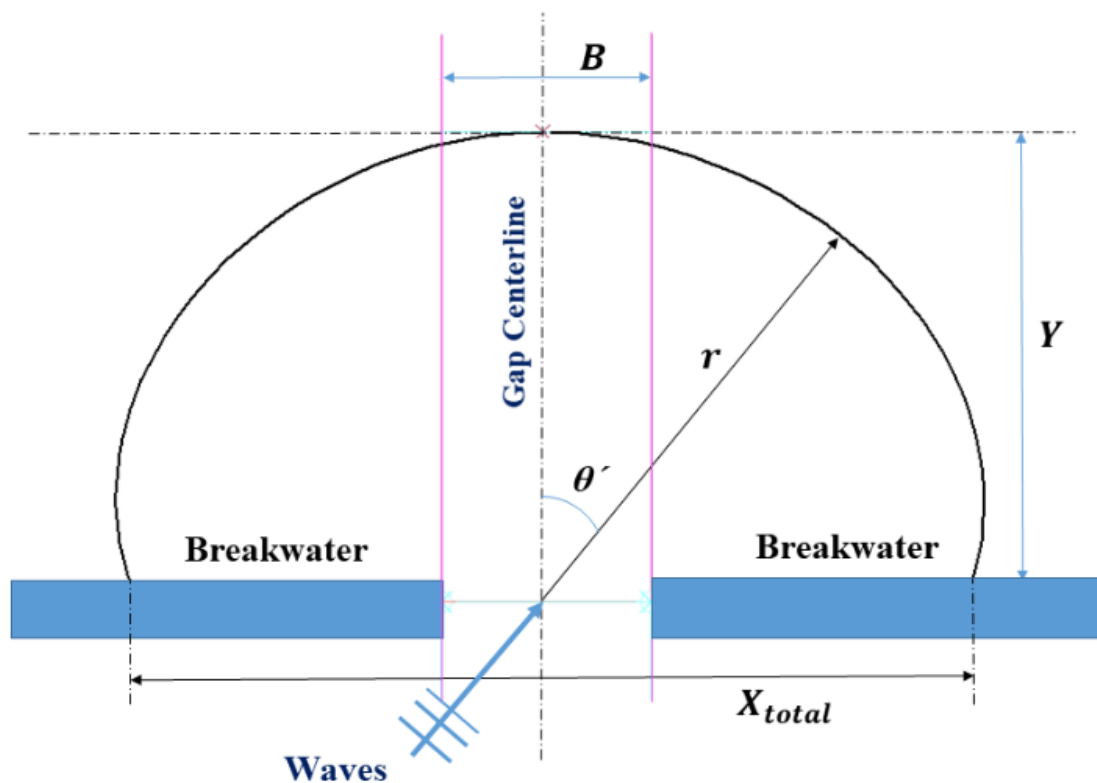
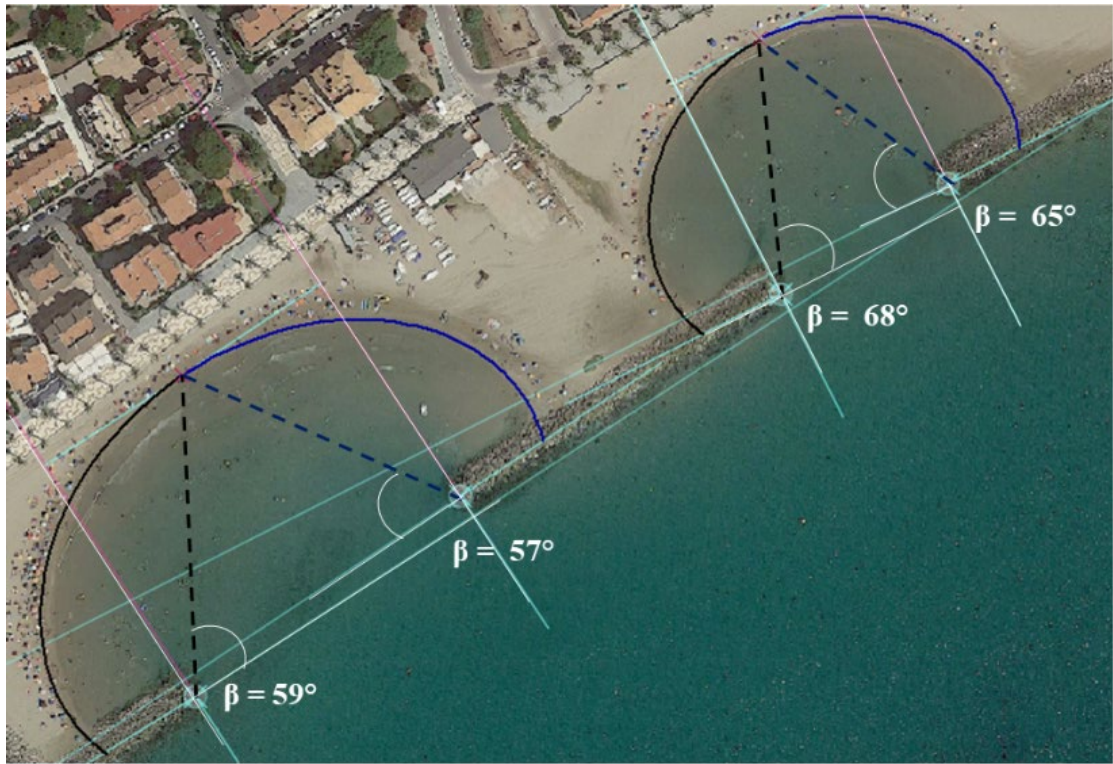
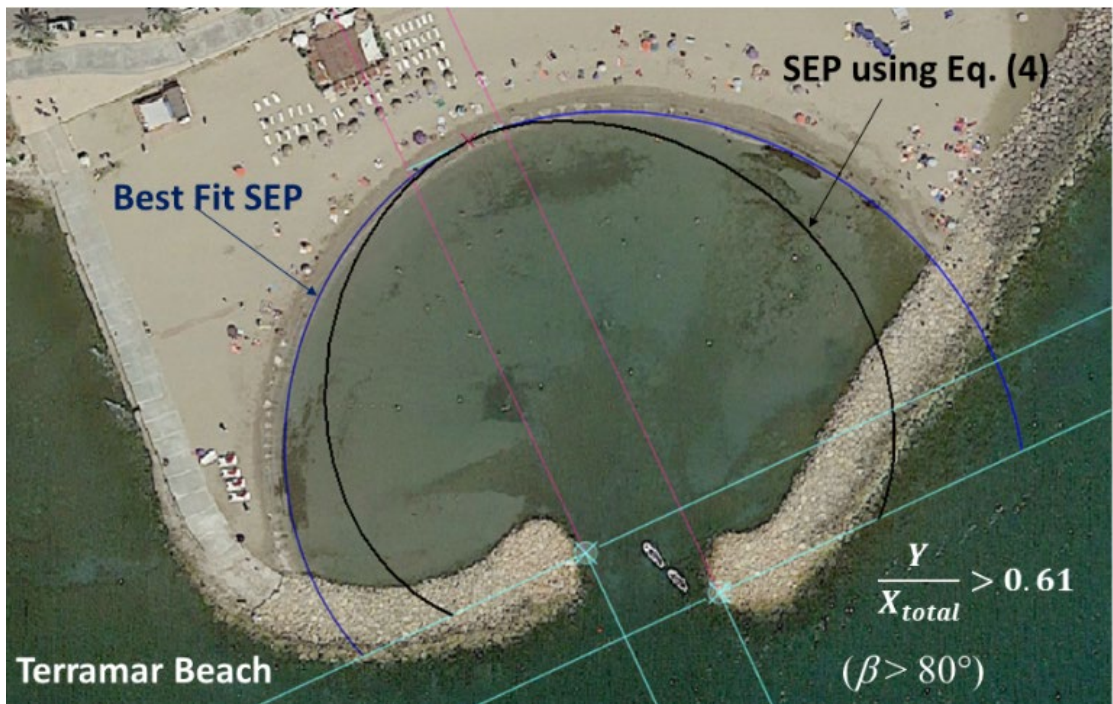
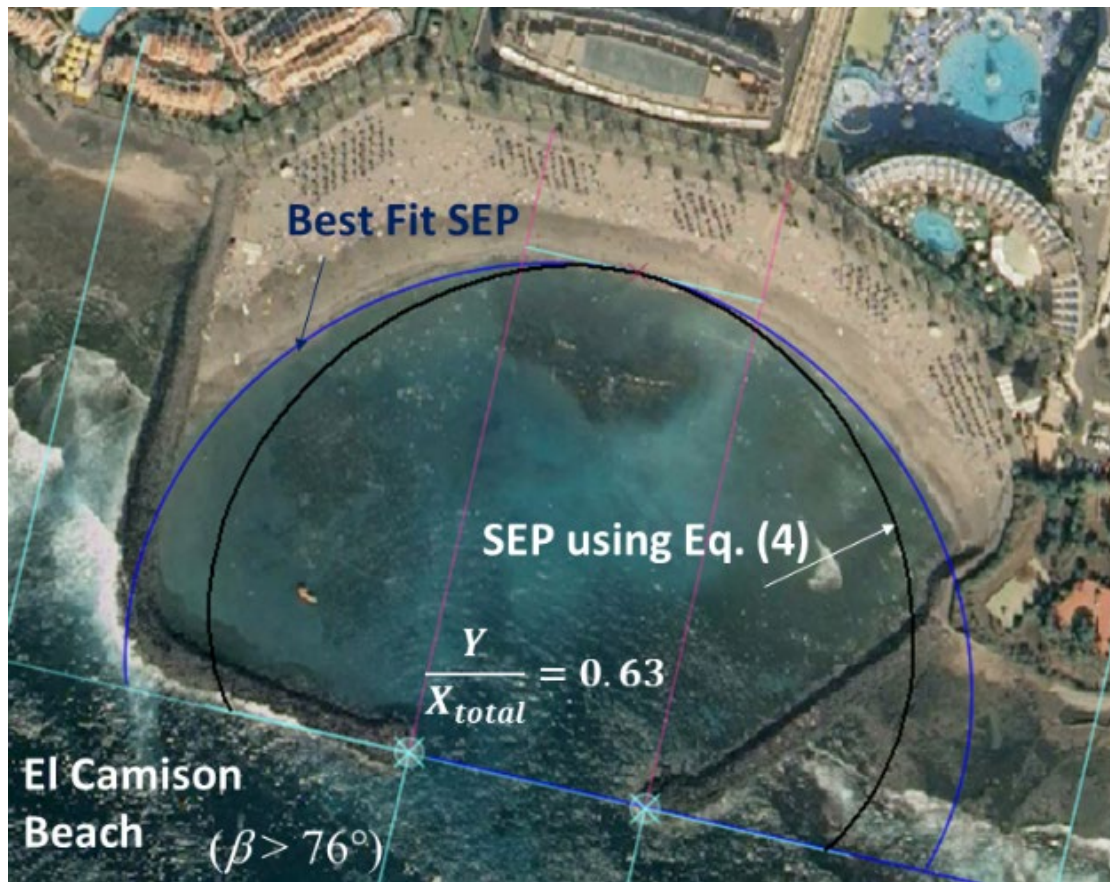


Fig. 2. Definition sketch of the planform of a bay formed on the leeward side of a breakwater gap, clarifying the maximum indentation ratio (Y/X_{total}) proposed by Silvester and Hsu (1997).



(a)





(b)

Fig. 3. (a) The static equilibrium planform, plotted using Eq. (4), of two pocket beaches at Lraga, Spain with obliquity angles ($\beta < 75^\circ$). (b) Examples of plotting the best-fitting SEP shapes and the SEP obtained using Eq. (4) for the beaches at Terramar and El Camison, which are characterized by large obliquity angles ($\beta > 75^\circ$). Photos are based on Google Earth imagery.

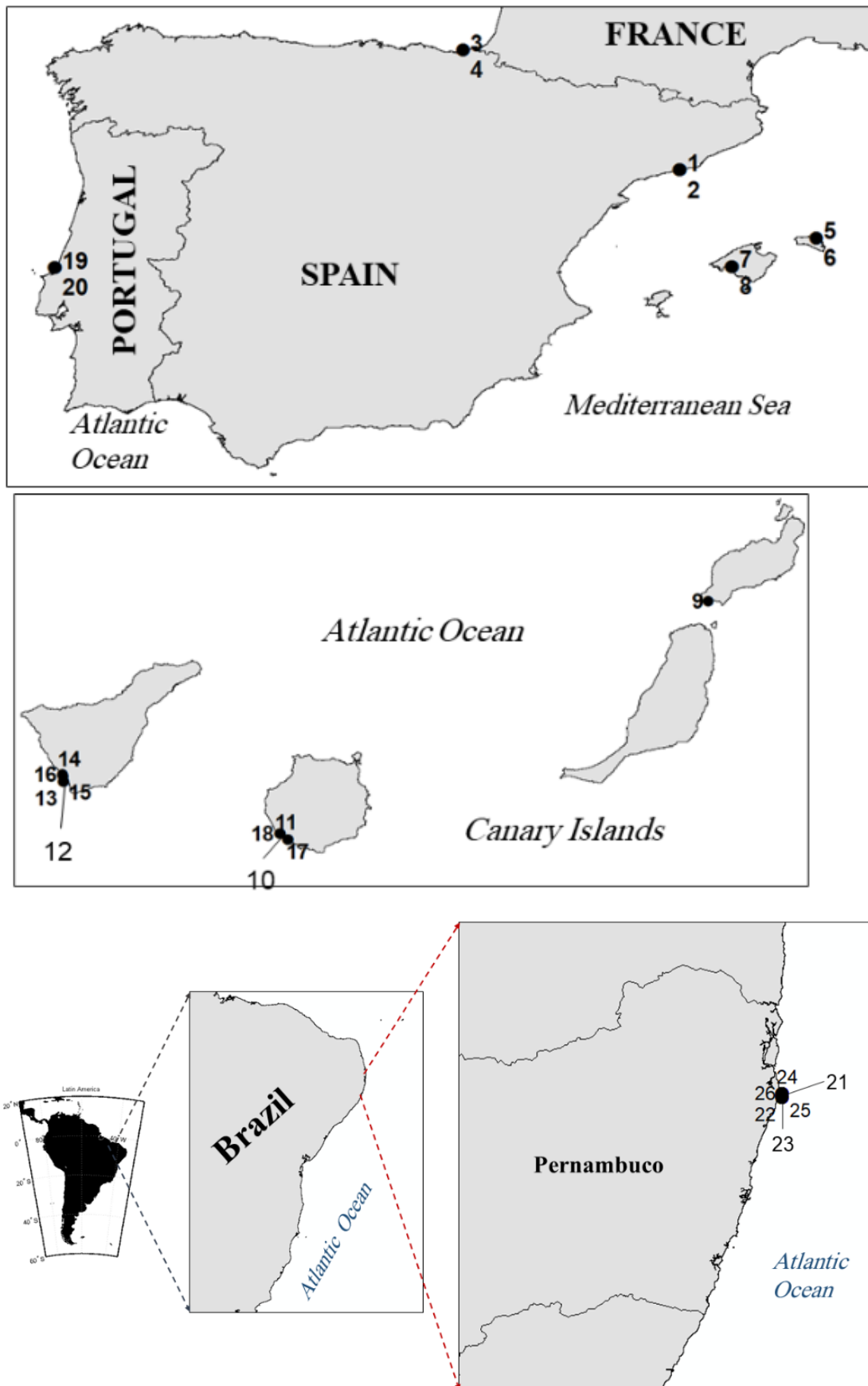


Fig. 4. Locations of the selected bay beaches in static equilibrium along the Iberian Peninsula coasts (upper and middle panels) and the Brazilian coast (lower panel).

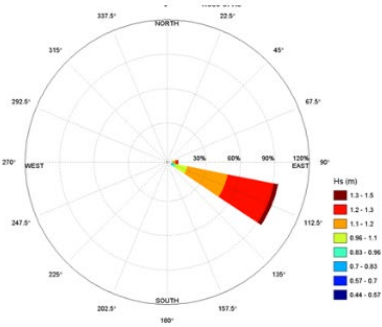
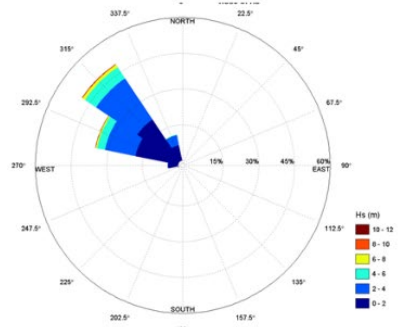
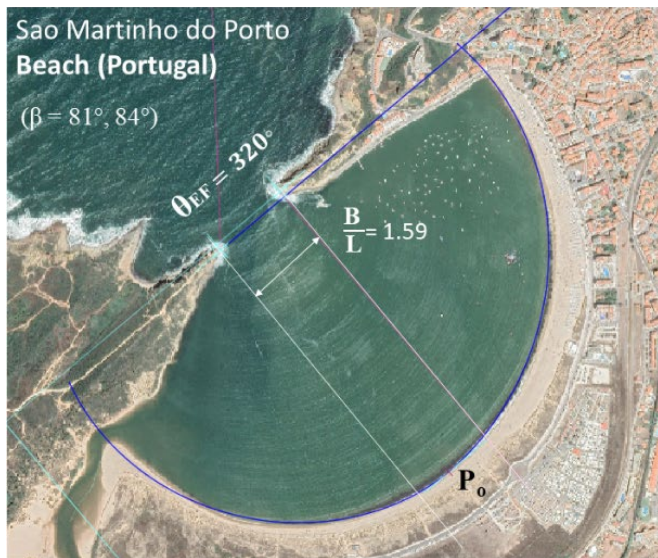
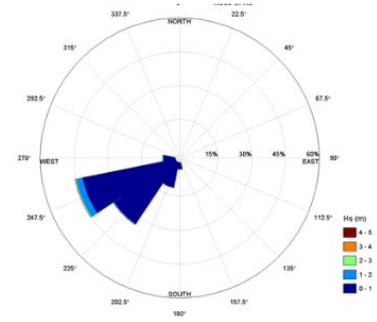
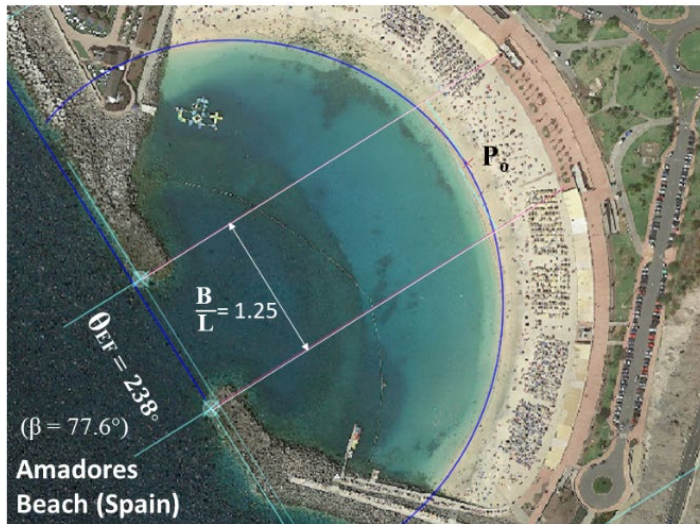


Fig. 5. Examples of the best-fitting SEP of the beaches at Amadores, Spain (upper panel), Sao Martinho do Porto, Portugal (middle panel) and Janga, Brazil (lower panel). Wave roses are plotted for a wave climate time series of more than 70 years (from 1948 onwards) using the DOW database. Photos are based on Google Earth imagery.

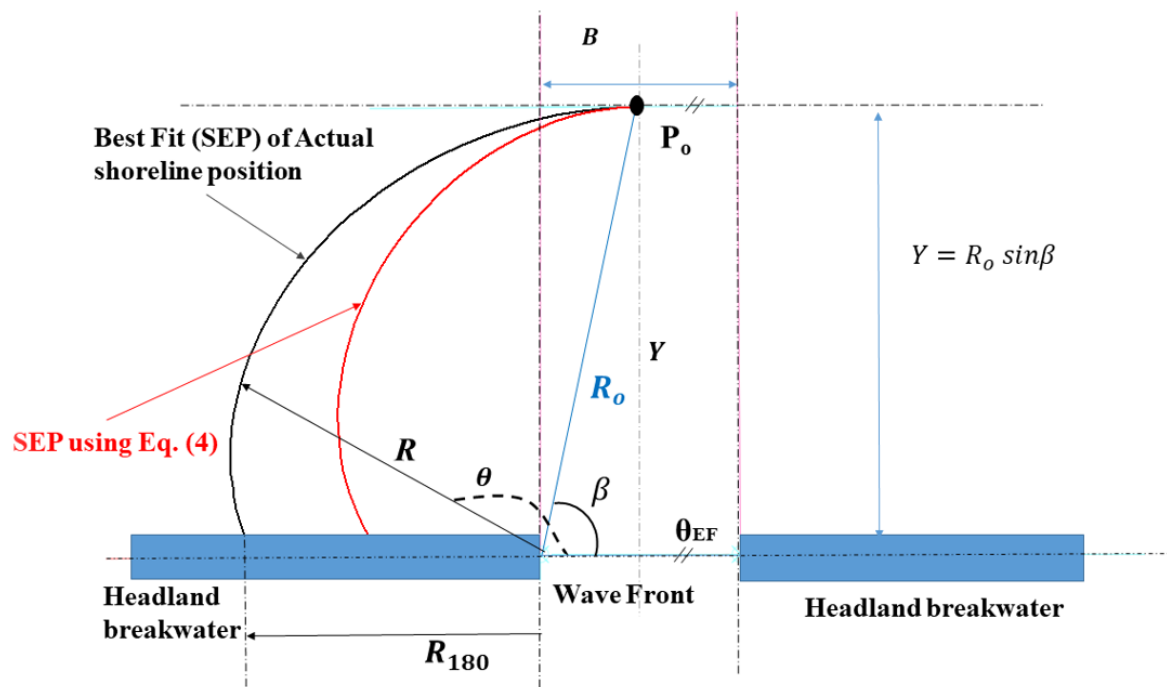


Fig. 6. Definition sketch of both the best-fitting SEP and the SEP obtained using Eq. (4). The obliquity angle (β) is the angle between the wave front corresponding to the direction of the wave mean energy flux (θ_{EF}) at the diffraction point and the control line (R_o).

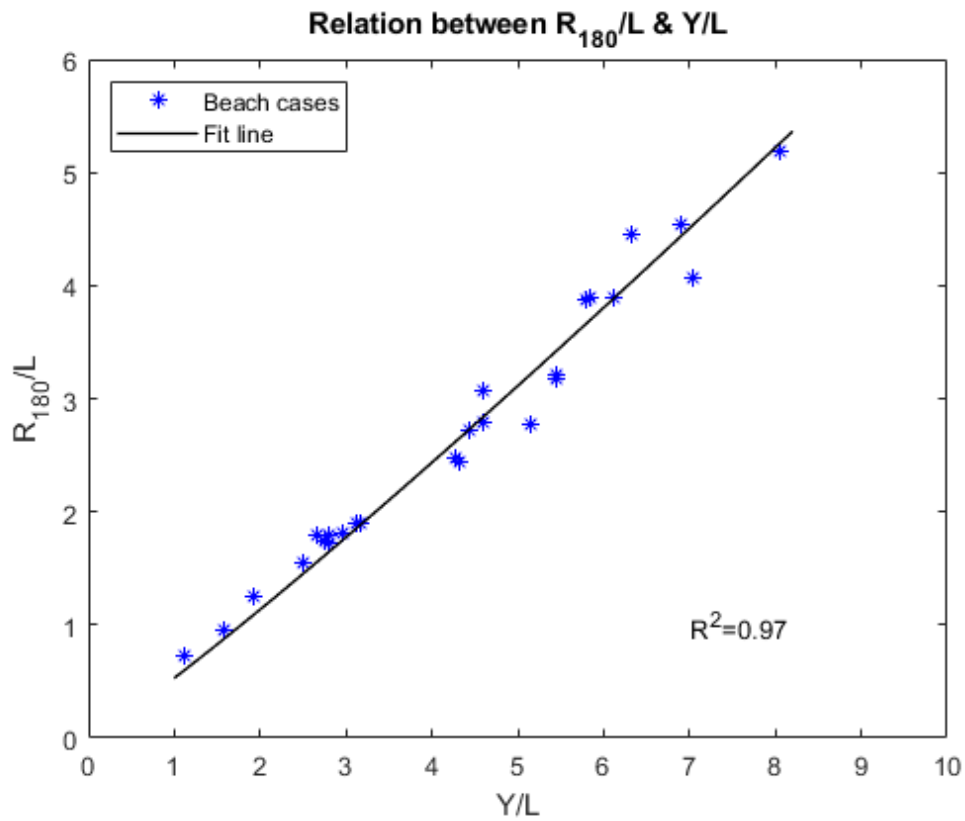


Fig. 7. Relation between the dimensionless distances (R_{180}/L) and (Y/L). The points represent the results of the best-fitting SEP based on the field observations, whereas the line represents the line of best fit obtained based on the regression analysis.

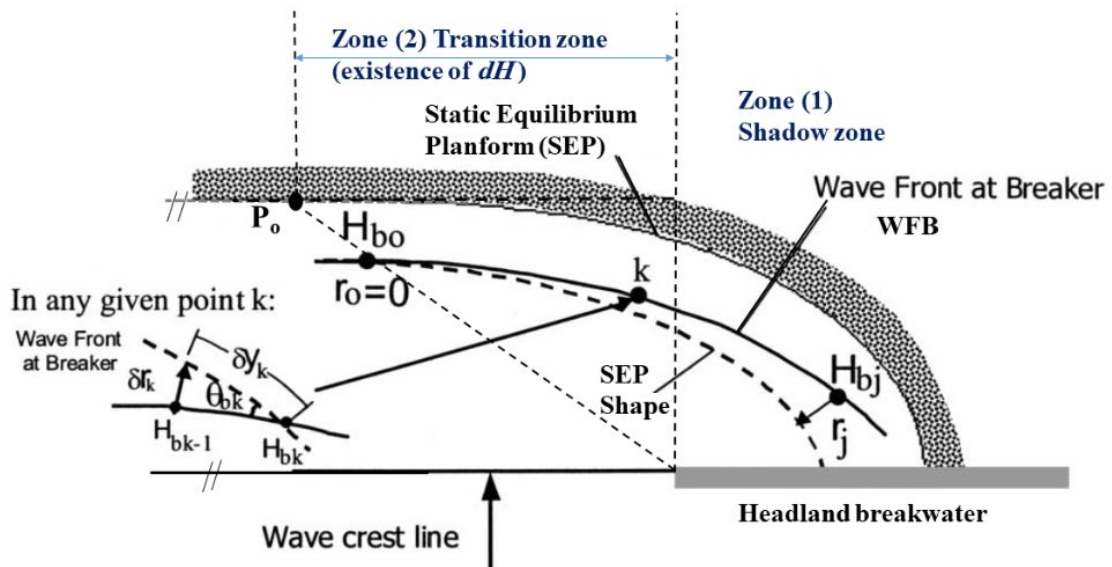


Fig. 8. Definition sketch of the static equilibrium shape in the planform of a bay beach and the Wave Front at Breaking (WFB), showing the transition and shadow zones on the leeward side of a headland breakwater, modified from González and Medina (2001).

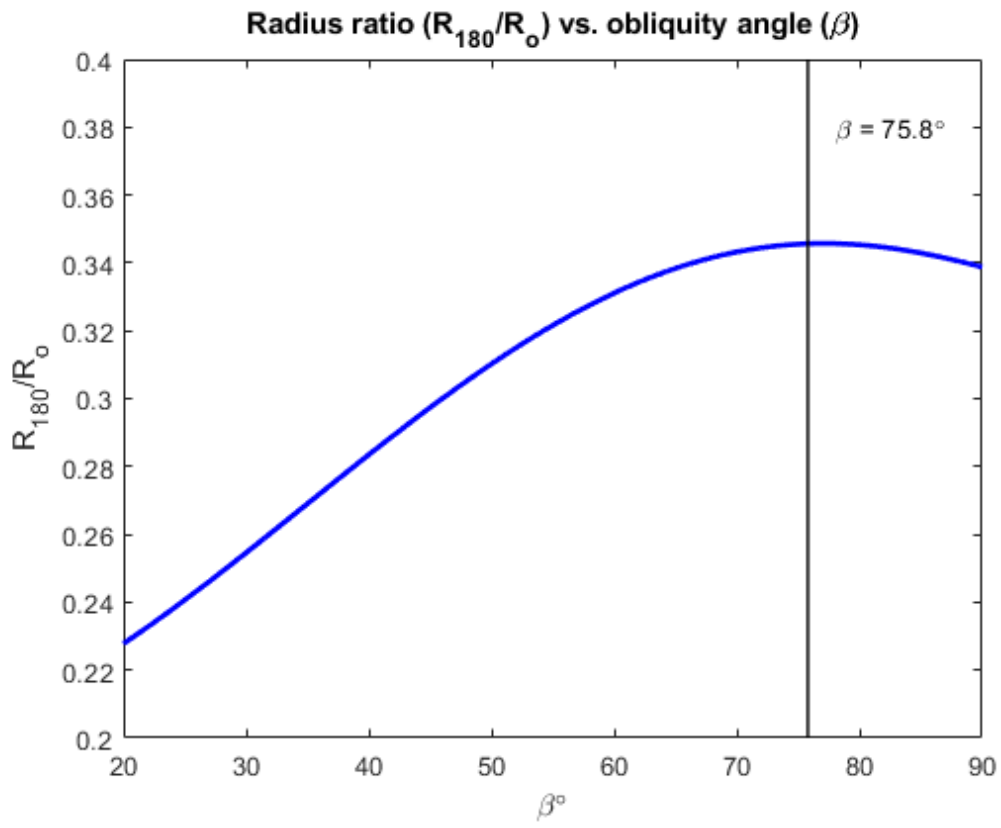


Fig. 9. The radius ratio (R_{180}/R_o) vs. the obliquity angle (β) for Eq. (4).

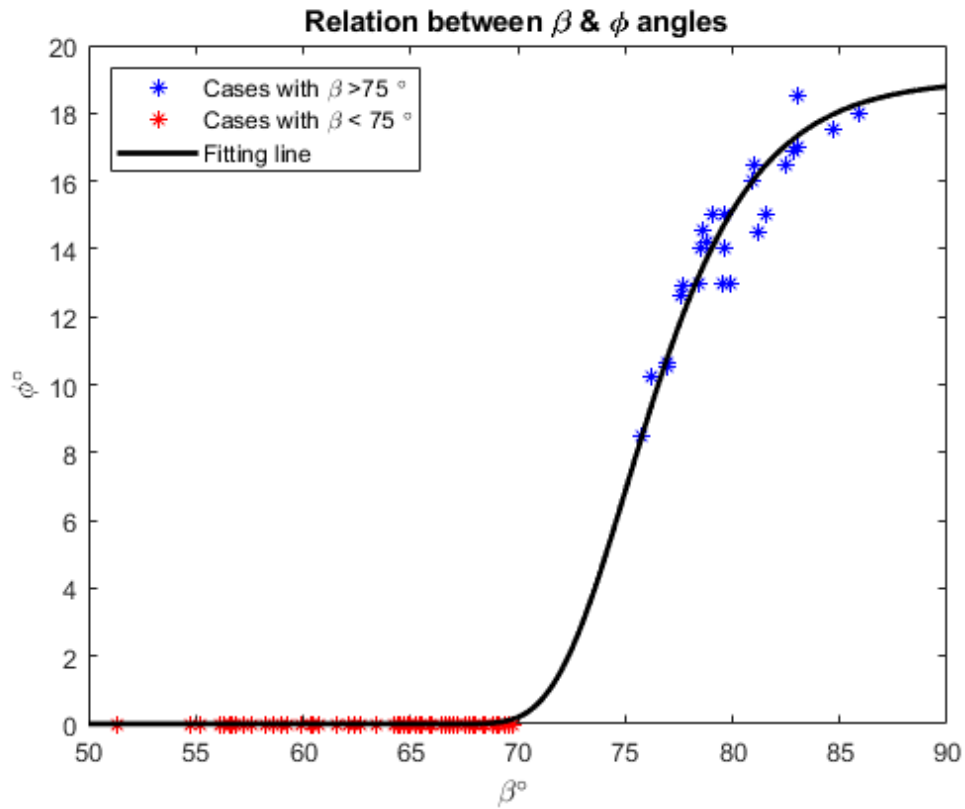


Fig. 10. Relation between the curvature-adjustment angle (ϕ) and the obliquity angle (β). The points represent the results of the best-fitting SEP obtained based on the field observations, whereas the line represents the line of best fit obtained based on the regression analysis.

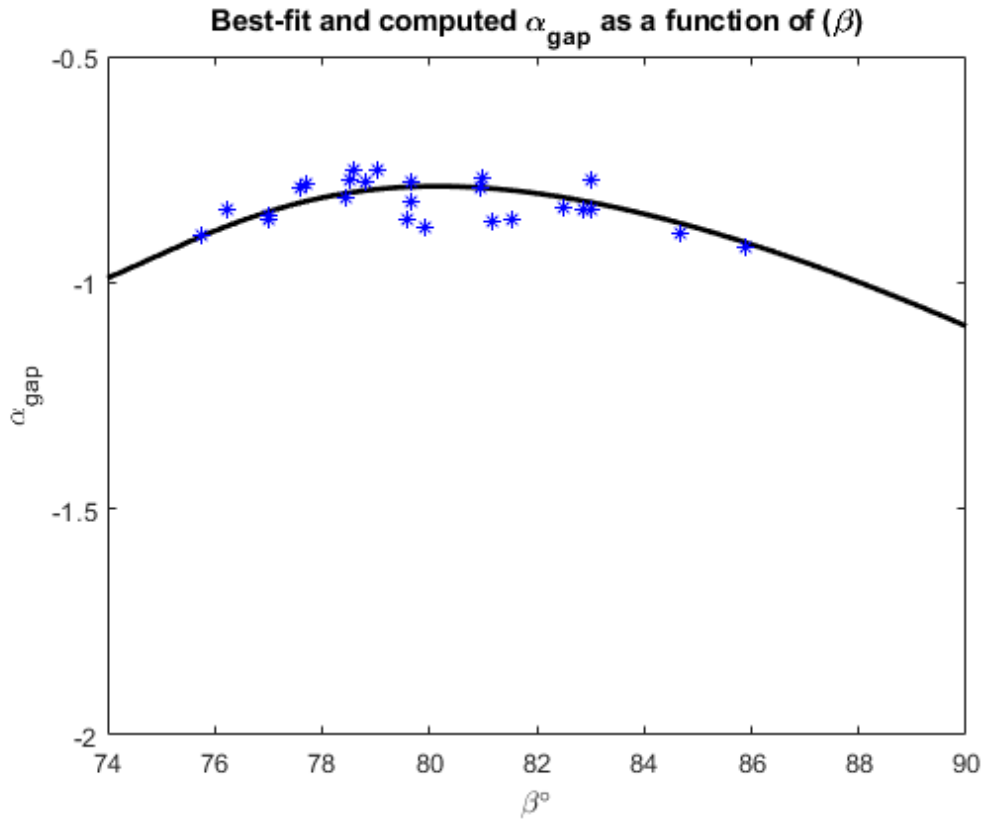


Fig. 11. The (α_{gap}) parameter as a function of the obliquity angle (β). The points represent the results of the best-fitting SEP based on the field observations of beach cases with ($\beta > 75^\circ$), whereas the line represents the proposed formula defined as Eq. (13).

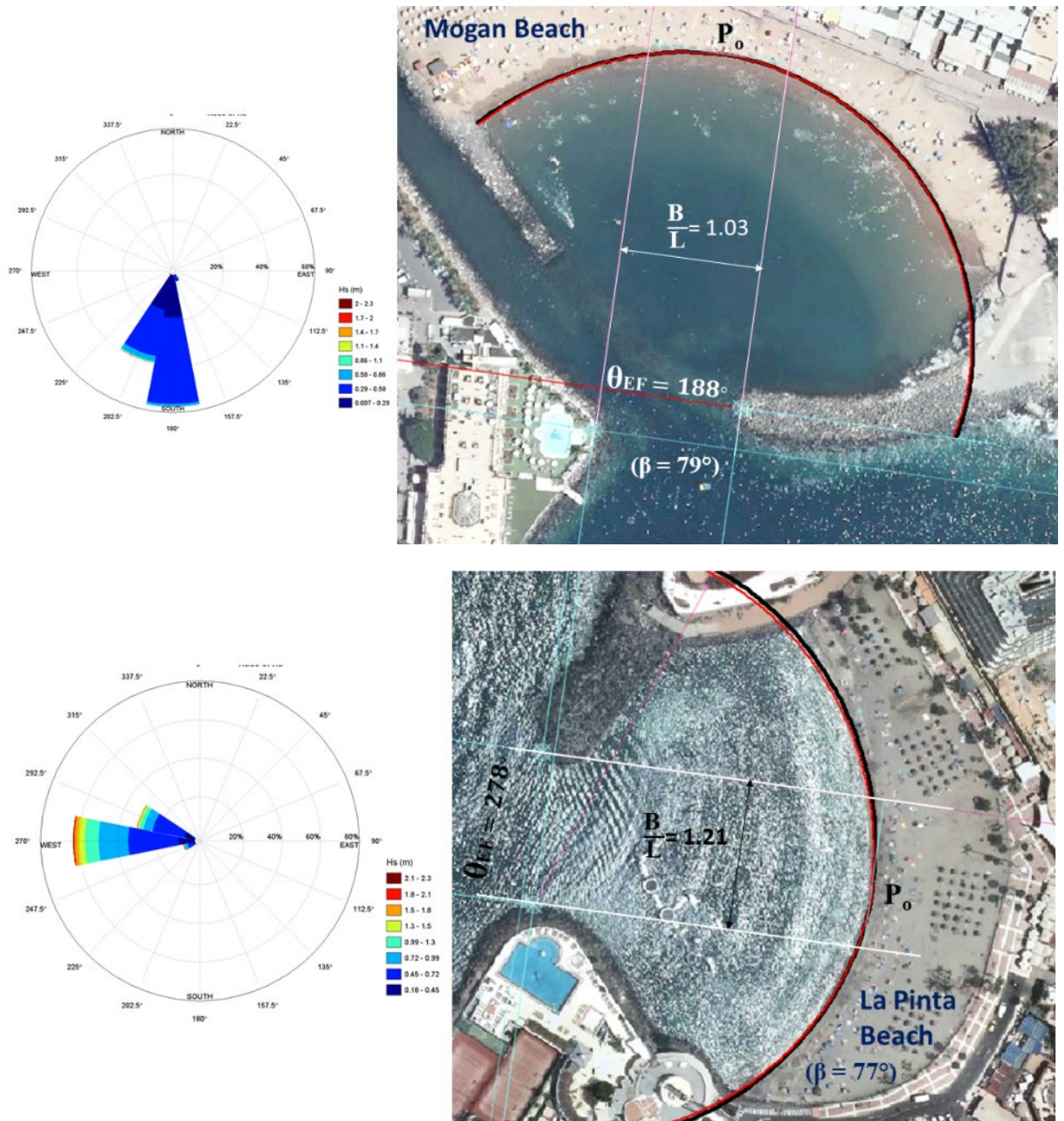


Fig. 12. Examples of plotting the best-fit static equilibrium planform (SEP) shape, in black, as well as the SEP obtained when applying Eq. (18), in red, for the beaches at Mogan (upper panel) and La Pinta, Spain (lower panel). Wave roses are plotted for a wave climate time series of more than 70 years (from 1948 onwards) using the DOW database. Photos are based on Google Earth imagery.